

Corrosion behaviour of copper alloys in natural sea water and polluted sea water

H. Le Guyader, A.M. Grolleau, V. Debout
DCNS CHERBOURG-CETEC -Code 0981 BP 440
50 104 CHERBOURG OCTEVILLE France

J.L. Heuzé, J.P Pautasso
DGA/DET/CEP
7-9 rue des Mathurins
92 220 BAGNEUX

ABSTRACT

Copper based alloys are frequently used in marine water systems. They have indeed an attractive price and offer interesting mechanical characteristics associated to a relatively good resistance to corrosion in sea water. Nevertheless, they can suffer from certain forms of corrosion such as localised corrosion with sulphides pollution, crevice corrosion, or stress corrosion cracking in sea water more or less polluted with ammonia.

A high strength copper nickel alloy (Nibron) and a Nickel Aluminium Bronze (A45) are respectively compared to classical CuNi 90-10 (CuNi10Fe1Mn) and CuAl9Ni3Fe2, elsewhere well known for their experimental feedback in sea water.

Standard electrochemical tests such as polarization resistance, open circuit potential measurements and polarization curves are implemented in natural sea water and polluted sea water. Static and under fretting crevice corrosion tests as well as specific stress corrosion cracking tests with ammonia pollution are also conducted.

The copper alloys compared have shown rather similar behaviour in sea water. In near stagnant conditions, risk of corrosion initiation in sea water is high with these alloys (localised corrosion, crevice corrosion close to the gasket, corrosion under deposit, stress corrosion cracking).

Usual recommendations for the use of copper alloys in sea water (ie passivation in clean sea water, suitable range of flow rate, biocide treatment) must be strictly followed in order to limit localised corrosion.

KEYWORDS: corrosion tests, copper alloys, natural sea water, polluted sea water

INTRODUCTION

Copper based alloys are frequently used in sea water system for applications such as heat exchangers, pumps, valves, pipes, fasteners. Depending on the applications and the need for mechanical characteristics, CuNi alloys (ie CuNi10Fe1Mn) or Nickel Aluminium Bronzes can be used. Despite the emergence in recent years of other materials that offer improved properties such as stainless steels, based nickel alloys or titanium, copper alloys continue to be widely used. They have indeed an attractive price and offer interesting mechanical characteristics associated to a relatively good resistance to corrosion in sea water. Nevertheless, they can suffer from certain forms of corrosion such as localised corrosion with sulphides pollution [1-6], crevice corrosion in valves or flanges assemblies [7-9]. Some cases of stress corrosion cracking in sea water more or less polluted with ammonia were also reported [10-12].

This paper summarises the results of a comparative test campaign conducted in natural sea water and polluted sea water on a high strength copper nickel alloy (Nibron compared to the classical CuNi10Fe1Mn) and a Nickel Aluminium Bronzes (A45 compared to CuAl9Ni3Fe2). Nibron and A45 being dedicated for fastener applications.

The following classical electrochemical tests were first conducted in natural sea water to assess corrosion parameters in the absence of critical interface:

- Open circuit potential (E_{oc}) and polarization resistance (R_p)
- Anodic polarization curves
- Weight loss measurements and corrosion rates estimation.

Secondly, the influence of sulphide or ammonia pollutions was investigated through the same approach.

Thirdly, critical interface that simulated flanges assemblies were considered and tested through crevice corrosion potentiostatic tests with a potential imposed close to E_{oc} .

Then, as relative micro displacements could be generated in certain assemblies, comparative tests regarding crevice corrosion initiation under fretting were also carried out.

Finally, as NAB could be susceptible to Stress Corrosion Cracking (SCC) in natural sea water or polluted sea water with ammonia, SCC U-bend tests were conducted.

EXPERIMENTAL PROCEDURE

Materials

Nominal compositions and mechanical properties of the base materials used are found in tables 1 and 2 with reference to certificate data, but also to analysis and mechanical tests conducted by the CESMAN¹ depending on the material considered.

Specimens conditioning

All specimens used were wet polished to a final finish with 600-grade SiC paper except SCC specimens that were polished to a 240-grit finish, degreased in methanol, rinsed in deionised water and then air dried. Prior to testing, all specimens were immersed in circulating natural sea water (2l/min) during about one month. Sea water is pumped from Cherbourg harbour with the temperature varying from 17°C to 20°C during the period of tests.

¹CESMAN Centre d'Expertises des Structures et MATériaux Navals (de DCNS)

Corrosion testing

Eoc and Rp measurements

Eoc and Rp measurements were conducted on specimens machined from bars with a flag shape to enable electric connection out of them sea water, the dimensions being of 25 mm in length and 25 mm in width. Eoc was measured with respect to Saturated Calomel reference Electrode (SCE). Rp measurements were obtained with linear polarization data acquired using a potentiostat by imposing a small amplitude potential of 15 mV around Eoc. The sweep rate was 0.05 mV/s. Rp was taken as the slope of the $I = f(E)$ curve near Eoc. Triplicate specimens were weighted before immersion and after cleaning with descaling solvents. Comparisons were made in each case with control specimens. Weight loss measurements were used to estimate the corrosion rates in $\mu\text{m}/\text{year}$. Specimen examination was conducted before and after cleaning. Tests were conducted in natural sea water during about 3 months but also in polluted sea water with sulphides or ammonia. Sea water pollution was simulated through Na_2S addition of 10 ppm S^{2-} , in quiescent sea water (Contact time 30 min before recirculation) every day during 5 days. The results obtained in non polluted circulating sea water were compared to those in polluted sea water after about 3 months of test. Ammonia additions were considered as another possible pollution that can be encountered in stagnant conditions due to organic matter degradation. NH_4OH was then added to stagnant sea water up to 1700 ppm of NH_3 , renewed every 2 weeks during more than one month. The results obtained in stagnant sea water renewed every 2 weeks were compared to those in stagnant sea water polluted with ammonia.

Polarization curves

The anodic polarization curves were generated using a potentiostat, at a scan rate of 0.05 mV/s, from Eoc to 0.3 V vs. SCE. The tests were conducted on “flag specimen” of 25 mm in length and 25 mm in width. Conditions of tests were the same as those selected for Eoc measurements.

Static crevice corrosion tests

The crevice device, shown in fig 1, was used in order to simulate metal /gasket interfaces such as flanges assembly under static conditions. The gaskets were aramid fiber gaskets and the assemblies were tightened to a controlled torque of 25 N.m leading to a pressure about $20 \text{ N}/\text{mm}^2$. It was lower than in service pressure but considered as a significant condition. One of the metallic surface was enlarged to enable crevice initiation out of the interface as it was generally observed in service. Potentiostatic tests, at ambient temperature, were conducted during 73 days in circulating natural sea water under an imposed potential chosen close to the Eoc measured.

Crevice corrosion tests under fretting

Assemblies used for crevice corrosion testing assisted by fretting consisted of three specimens with cylindrical bosses fastened through their central hole with a controlled pressure of $2 \text{ N}/\text{mm}^2$ as shown in figure 2. The tests were performed in natural sea water at a controlled temperature of 25°C . Micro-displacements of 10 microns were generated at a frequency of 10 Hz for 2 or 3 hours. Potentiostatic tests were conducted increasing the potential step by step. The first phase consist of waiting for steady current close to Eoc potential, then implementing a fretting sequence and recording the corresponding current. Then, potential was increased and the fretting sequence implemented. This step was repeated until the current reached 10^{-4} to 10^{-3} Amps.

Stress corrosion cracking tests

U-Bend tests were conducted according to ISO 7539-3 standard (ref 13). Tests parameters were selected with regard to those defined previously to estimate CuAl9Ni3Fe2 SCC susceptibility in natural sea water and polluted stagnant sea water with aqueous ammonia [14]. Specimens were bent to a bending radius of 14 mm. Test environments chosen were natural sea water and stagnant sea water added with two concentrations of aqueous ammonia: 170 ppm (0.01 mol/l) and 1700 ppm (0.1 mol/l). Cracks were indeed observed on CuAl9Ni3Fe2 in these conditions after respectively 1000 h and 120 h of test duration (ref 14). Each specimen was duplicated and two test durations were selected, 1000 hours and 5000 hours (four specimens tested in each condition).

RESULTS AND DISCUSSION

Corrosion parameters in natural sea water (absence of critical interface)

Eoc measurements of Nibron compared to CuNi10Fe1Mn are given in Figure 3. In natural sea water, Nibron Eoc is maintained around -250 mV vs. SCE over a period of time of about one month. Then, Eoc increases to -70 mV vs. SCE after 2 months of test. The triplicate specimens in test give the same results.

Rp measurements of Nibron, shown in Figure 4, confirms this tendency to corrosion initiation with an initial value of 5000 to 10 000 Ohm decreasing to between 10 and 300 Ohm after 2 months of exposure to sea water. Nibron specimens examinations, presented in Figure 5, shows green oxidation products significant of corrosion initiation. The mean corrosion rate is nevertheless low around 18 $\mu\text{m}/\text{year}$. Pitting corrosion is observed but the pit depths are too low to be estimated. After one month of exposure to natural sea water, anodic polarization curves, in Figure 6, exhibit no actual passivation threshold, the current density increases from $10^{-7} \text{ A}/\text{cm}^2$ to about $10^{-5} \text{ A}/\text{cm}^2$ up to a potential of -50 mV vs. SCE. Over this potential, anodic current sharply increases to $10^{-3} \text{ A}/\text{cm}^2$. If Nibron is compared to the classical CuNi10Fe1Mn, mean corrosion rate could be considered similar respectively 18 $\mu\text{m}/\text{year}$ and 15 $\mu\text{m}/\text{year}$ but Nibron could have a higher tendency to pitting in natural sea water. Eoc and Rp measurements confirm this different behaviour. CuNi10Fe1Mn presents indeed a steady potential and Rp with time, respectively -200 mV vs. SCE and 2000 Ohm as Nibron shows an increase in potential over -100 mV vs. SCE and a decrease in Rp under 100 Ohm after 2 months of exposure to sea water.

In conclusion, Nibron could be considered a bit more susceptible to corrosion and especially localised corrosion than CuNi10Fe1Mn in natural sea water.

Eoc measurements of A45 compared to the NAB CuAl9Ni3Fe2 are given in Figure 7. Similar phenomenon is observed on both alloys, that is an increase in potential from -250 mV vs. SCE to -90 mV vs. SCE after 2 months of exposure to sea water. At the same time, Rp shown in Figure 8, presents similar evolution with a decrease from a steady value of 3000 Ohm to 100 Ohm after 2 months of test. Specimen examinations reveal a mean corrosion rate of 37 $\mu\text{m}/\text{year}$ with a localised corrosion observed near the coated electric connection evaluated at 1.3 mm/year, the max. depth being of about 150 to 300 μm . Similar observations are made on CuAl9Ni3Fe2. Anodic polarization curves performed on A45 and CuAl9Ni3Fe2, in Figures 9 and 10, are very similar. No actual passivation thresholds are observed in both cases. For A45, current densities increase slowly from $10^{-6} \text{ A}/\text{cm}^2$ to 10^{-5}

A/cm² between -220 mV vs. SCE and -100 mV vs. SCE. Then, over - 100 mV vs. SCE , current densities sharply increase to 10⁻³ A/cm².

In conclusion, electrochemical behaviour of A45 and CuAl9Ni3Fe2 are very similar with a higher tendency to localised corrosion of these both alloys compared to Nibron or CuNi10Fe1Mn.

Influence of sulphides pollution on corrosion parameters

With sulphides pollution, Eoc measured on Nibron shown in Figure 3 increases from - 250 mV vs. SCE to -70 mV vs SCE after 2 months of test, as it was observed in natural sea water. At the same time Rp , in Figure 4, decreases to 100 Ohm. Specimen examination after the test, reveals an important green oxides deposit as shown in Figure 5 with a mean corrosion rate estimated about 49 µm/year. Nibron anodic polarization curve with sulphides pollution is very similar to those of CuNi10Fe1Mn. Anodic current, in Figure 6, sharply increases to 10⁻⁴ A/cm² for a potential between -100 mV vs. SCE and -30 mV vs. SCE.

In conclusion, with sulphides pollution, Nibron presents a comparative behaviour to CuNi10Fe1Mn. Compared to results in natural sea water, mean corrosion rates are increased and affected areas are spread all over the exposed surface in both cases.

Influence of ammonia pollution on corrosion parameters

With ammonia pollution, A45 Eoc, shown in Figure 11, decreases from - 250 mV vs ECS to -350 mV vs. ECS. This decrease in potential was checked on Pt Electrode. The same phenomenon is also observed on CuAl9Ni3Fe2 (see Figure 12). Specimen examinations after the tests reveal a superficial corrosion with no significant pitting. The mean corrosion rates for A45 and CuAl9Ni3Fe2 are respectively 13 µm/year and 16 mm/year. Anodic polarization curves performed on A45 and CuAl9Ni3Fe2, in Figure 9 and 10 reveal a significant increase in current between -150 mV vs. SCE and - 250 mV vs. SCE in sea water with ammonia pollution. The current densities reach 7.10⁻⁵ A/cm².

In conclusion, these tests reveal the potential risk of galvanic coupling between a surface polluted with ammonia and a large surface in unpolluted natural sea water.

Parameters of crevice corrosion initiation (Static tests) in natural sea water

Tests conducted on Nibron, under - 70 mV vs ECS in Figure 13, lead to a high current around 10⁻³ A/cm² after 100 hours of test. A uniform corrosion is observed, localised out of the crevice interface. CuNi10Fe1Mn presents exactly the same phenomenon with lower current about 5. 10⁻⁵ A/cm² under a potential of -75 mV vs. ECS.

On A45, the current measured under - 100 mV vs SCE is 10⁻⁵ A/cm² after 100 hours of test. Then, it increases gradually to 10⁻⁴ A/cm² (see Figure 14). Corrosion is observed out of the crevice interface but localised at the edge of the gasket. A45 and CuAl9Ni3Fe2 show a very similar behaviour.

In conclusion, the various materials tested show a certain susceptibility to crevice corrosion. In each case, this corrosion is localised out of the crevice interface and close to the gasket edge in the case of NAB.

Parameters of crevice corrosion initiation and propagation under fretting in natural sea water

On the Nibron crevice device, tests begin under a potential of -150 mV vs. SCE. As shown in Figure 15, currents are maintained low (10^{-6} A) for a potential varying from -150 mV vs SCE to -100 mV vs SCE. Above these potential, currents become significant from -70 mV vs SCE and reach $8 \cdot 10^{-4}$ A. Fretting induces no significant increase in current. For imposed potentials from -60 mV vs. SCE to -50 mV vs. SCE, corrosion currents are very high ($2 \cdot 10^{-3}$ A). After the tests, specimen examination, presented in Figure 16, reveals superficial corroded areas at the periphery and corrosion initiates near the hole but this corrosion has occurred during the initial immersion phase but not during the fretting step.

A comparative test conducted on CuNi10Fe1Mn with the results shown on Figure 17 and 18 leads to the same conclusions with no significant effect of the fretting observed. Initiation potential is estimated around -70 mV vs. SCE under static conditions as under fretting. Corrosion areas are also mainly located at the periphery of the specimen.

On A45 (see Figure 19), corrosion initiates naturally under free potential (-105 mV vs. SCE) at the beginning of the test. Under -100 mV vs. SCE, the current reaches $2 \cdot 10^{-4}$ A which is higher than those observed on Nibron and CuNi10Fe1Mn in the same conditions. Under -80 mV vs. SCE, fretting has got an effect on the current measured: after a fretting step of about one hour, corrosion current increases from $4.4 \cdot 10^{-4}$ A to $6.2 \cdot 10^{-4}$ A. From -70 mV vs SCE, the current measured become very high (10^{-3} A) but similar under static conditions and under fretting. Specimen examination, shown on Figure 20, reveals after the fretting test a selective corrosion at the periphery of the specimen with dealuminisation, the maximum corrosion depth being of 0.1 mm.

The comparative test conducted on CuAl9Ni3Fe2, in Figures 21 and 22, leads to similar observations with lower currents measured. Under -100 mV vs. SCE, the current measured is indeed 9 fold higher on A45. In both cases, A45 and CuAl9Ni3Fe2, fretting begins to be effective from -80 mV vs SCE with high steady currents that reached respectively $6.2 \cdot 10^{-4}$ A and $2.8 \cdot 10^{-3}$ A. The crevice corrosion test under static conditions previously presented, seems to be less severe with corrosion current measured around 10^{-4} A under a potential of -100 mV vs. SCE.

In conclusion, initiation potentials in static conditions and under fretting are similar but fretting could have an effect on corrosion rates especially on A45 and CuAl9Ni3Fe2. Globally corrosion initiated naturally during the immersion phase and propagated under imposed potential essentially out of the crevice interface under fretting but also in static conditions.

U-bend SCC tests in natural sea water and polluted sea water with ammonia

On A45, cracks initiate in sea water polluted with 1700 ppm of ammonia after 1000 hours of tests as shown in Figures 23 and 24, but not in natural sea water and polluted sea water with 170 ppm of ammonia. By comparison, CuAl9Ni3Fe2, suffers from SCC in natural sea water and polluted sea water with only 170 ppm of ammonia. Experimental feedback presented previously [14] had confirmed the susceptibility CuAl9Ni3Fe2 in stagnant sea water in long term service conditions. The test in sea water polluted with ammonia was considered as one possible simulation of SCC phenomenon in stagnant sea water. In that conditions, A45 could be considered as susceptible to SCC in stagnant sea water but high concentrations of ammonia are needed to reveal its susceptibility compared to CuAl9Ni3Fe2 so that it appears less critical.

U-bend tests conducted on Nibron compared to CuNi10Fe1Mn, shown in Figures 25 and 26 has revealed no susceptibility of both alloys to SCC in natural sea water but also in stagnant sea water possibly polluted with ammonia after 5000 hours of tests.

CONCLUSION

A comparative test campaign was conducted in natural sea water and polluted sea water on a high strength copper nickel alloy (Nibron compared to the classical CuNi10Fe1Mn) and a Nickel Aluminium Bronzes (A45 compared to CuAl9Ni3Fe2). The following conclusions can be drawn from this study:

1. In natural sea water Nibron appears slightly more susceptible to corrosion than CuNi10Fe1Mn, A45 and CuAl9Ni3Fe2 have a similar behaviour considering electrochemical tests.
2. Sulphides pollution leads to a significant increase in corrosion on Nibron and CuNi10Fe1Mn.
3. NH₃ pollution increases the risk of SCC on A45 and CuAl9Ni3Fe2 as Nibron and CuNi10Fe1Mn show no susceptibility to this form of corrosion.
4. Presence of gasket increases the risk of crevice corrosion initiation near the gasket but not under the gasket, phenomenon more over observed in operating conditions.
5. Crevice corrosion initiation potentials are similar under static conditions and under fretting. For A45 and CuAl9Ni3Fe2, fretting could have an effect on corrosion rates, currents level are higher. Globally, corrosion can initiate naturally during the immersion phase in sea water and propagate under imposed potential essentially outside interface specially under fretting conditions but also in static conditions.

Globally, the copper alloys compared have shown rather similar behaviour. In sea water near stagnant conditions, risk of corrosion initiation is high with these alloys (localised corrosion, crevice corrosion close to the gasket, corrosion under deposit, stress corrosion cracking). Usual recommendations for the use of copper alloys in sea water (ie passivation in clean sea water, suitable range of flow rate, biocide treatment) must be strictly followed in order to limit localised corrosion.

ACKNOWLEDGMENTS

The authors will gratefully acknowledge J Mawella (from MoD) and J Galsworthy (from Qinetiq) for supporting the French/UK scientist exchange (British French Cooperation Program) which significantly enhanced this study. This work was funded by the French Ministry of Defence (DGA/DSA/SPN). B. Avaulée and E. Postaire are recognised for their efforts in conducting the tests. The authors also express their appreciation to the whole DCNS /CETEC/MCP staff for their participation to this work and like to thank JM Corrieu from CESMAN for assistance in material chemical analysis and mechanical evaluations.

REFERENCES

1. BC SYRETT, Sulfide attack in steam surface condensers, Conf on environmental degradation of engineering materials in an aggressive environment, Virginia Polytechnic Institute, 1981

2. AM BECCARIA, G POGGI, P TRAVERSO , A study of 70Cu30Ni commercial alloy in sulphide polluted and un polluted sea water, Corrosion Science vol 32, N°11, 1991, P1263
3. JN AL-HAJJI and MR REDA , The corrosion of copper nickel alloys in sulfide polluted sea water: the effect of sulfide concentration, Corrosion science Vol 34 n°1, 1993,p163
4. DR LENARD and RR WELLAND, Corrosion problems with copper nickel components in sea water systems , paper 599 , Corrosion 98
5. DR LENARD, The effect of decaying organisms on the corrosion of copper nickel alloys in sea water, paper 02185, Corrosion 2002
6. A KLASSERT, L TIKANA Copper and copper nickel alloys- an overview Eurocorr 2004
7. RM KAIN, BE WEBER, Effect of alternating sea water flow and stagnant layup conditions on the general and localized corrosion resistance of CuNi and NiCu alloys in marine service, paper 422, Corrosion 97,
8. AYLOR OM, HAYS RA, KAIN RM, Crevice performance of candidate naval ship sea water valve materials, paper 329 , Corrosion 99,
9. H HOFFMEISTER, J ULLRICH, Quantitative effect of transient potentials and temperature on crevice corrosion of Naval Cast CuNiAl Valve bronze in natural sea water Corrosion 2000
10. JOSEPH G , PERET R, OSSIO M , Copper and Al Cu Stress Corrosion in artificial sea water,10th international congress on metallic corrosion Vol V Madras India 8912-72-0599 pp185-197 DP 1989
11. G JOSEPH, Stress corrosion cracking susceptibility of alpha aluminium bronzes in sodium chloride solutions. 1-3 oct 1990 VASTERA CONGR CENTER 9103-72-0162 pp447-493 DP 1990
12. KUNIGAHALLI L VASANTH AND RICHARD A HAYS. Corrosion assessment of Nickel Aluminum Bronze (NAB) in sea water. Corrosion 2004 paper 04294.
13. ISO 7539-3-Corrosion of metals alloys-Stress corrosion testing-part 3: Preparation and use of U-bend specimens
14. H LE GUYADER, A.M GROLLEAU, JL HEUZE, V DEBOUT. Stress Corrosion Cracking susceptibility of Nickel Aluminium Bronzes in Natural Sea Water , Eurocorr 2005 , Paper 38 Lisbon

Material	Al	Zn	Ni	Fe	Mn	Impur	Si	Sn+Pb	P	C	S	Cu
Nibron According to CESMAN analysis	2.53	0.006	13.8	1.06	0.43		0.004	0.0010 (Pb)	<0.0 03	0.004	<0.001	82
CuNi10Fe1Mn Certificate data		0.006	10.5	1.7	0.87	0.04		0.004	0.015	0.009	0.005	Bal
A45 Certificate data	9.96	0.01	4.80	3.28	0.55	0.04	Nil	0.15 (Sn)				Bal (incl Ag)
CuAl9Ni3Fe2 Certificate data	8.8	0.01	2.7	2.1	1.37	0.04	0.03	0.02 (Sn) 0.001 (Pb)				Bal

Table 1: Chemical composition of the base metal alloys (% in weight)

Material	0.2% YS (MPa)	UTS (MPa)	Elongation %	Hardness Average value
CuNi10Fe1Mn Certificate data	129	320	42.6	90 (HB)
Nibron according to CESMAN tests	579	811	17.5	
CuAl9Ni3Fe2 Certificate data	251	576	54	137(HB)
A45 According to CESMAN tests	640	810	20	

Table 2: Mechanical properties of the base metal alloys

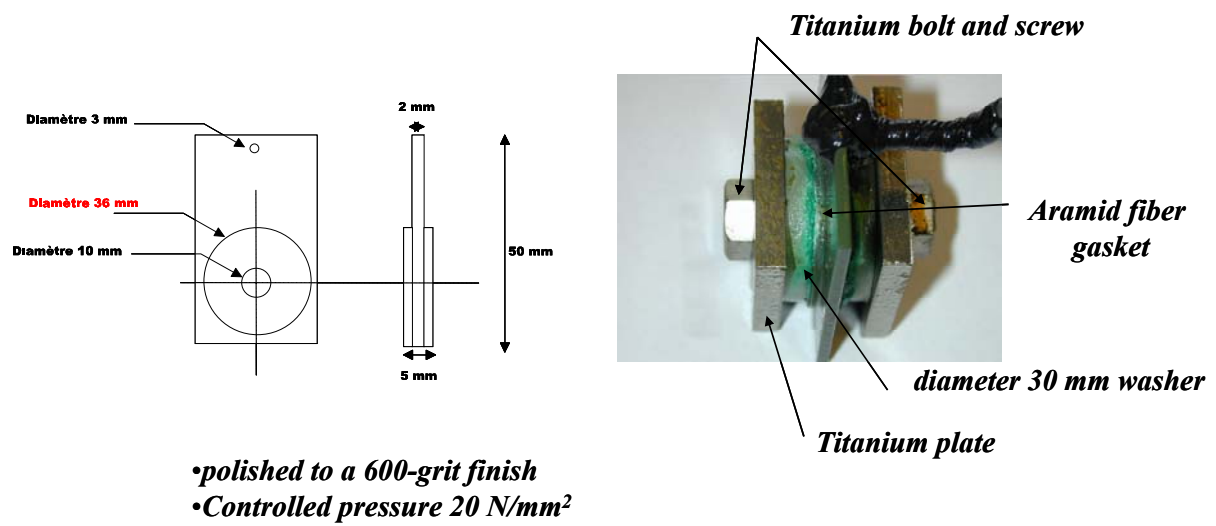


Figure 1 : Static crevice test device

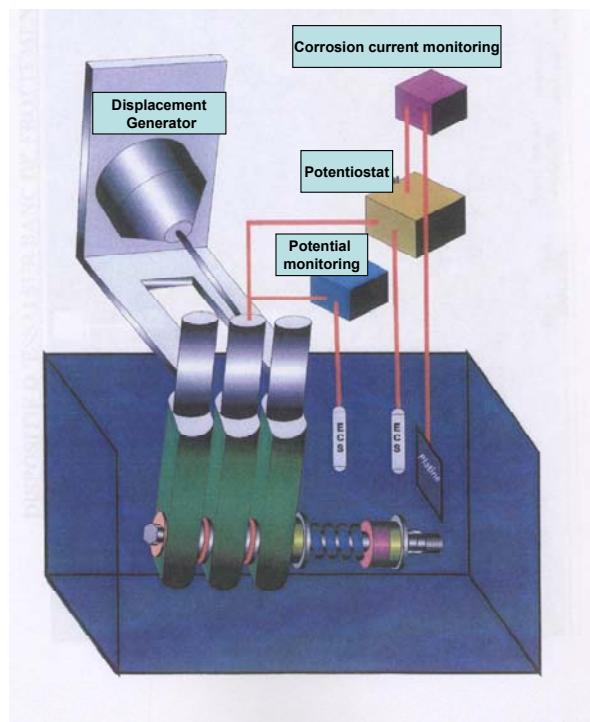
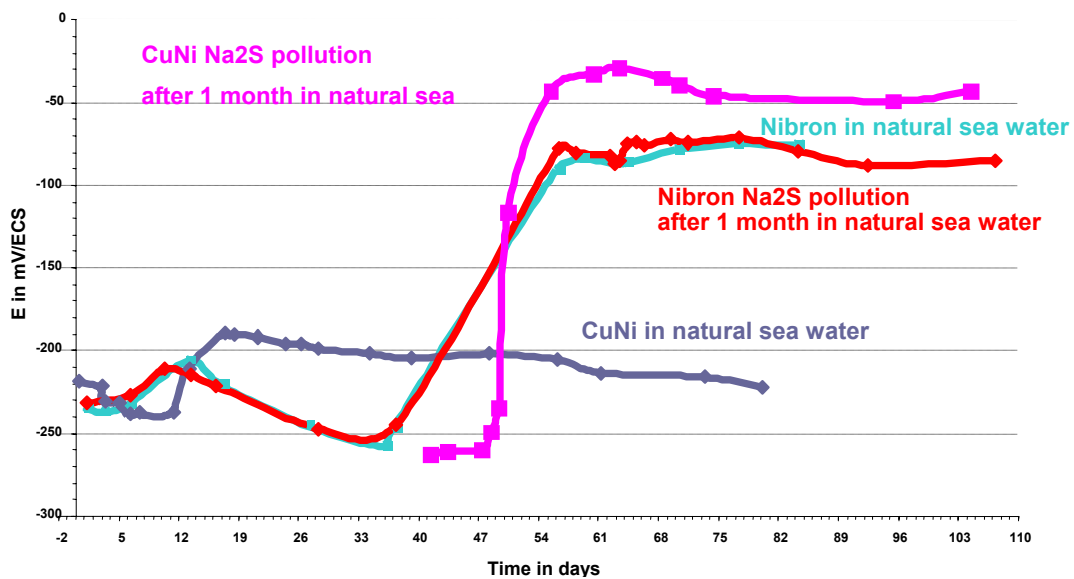
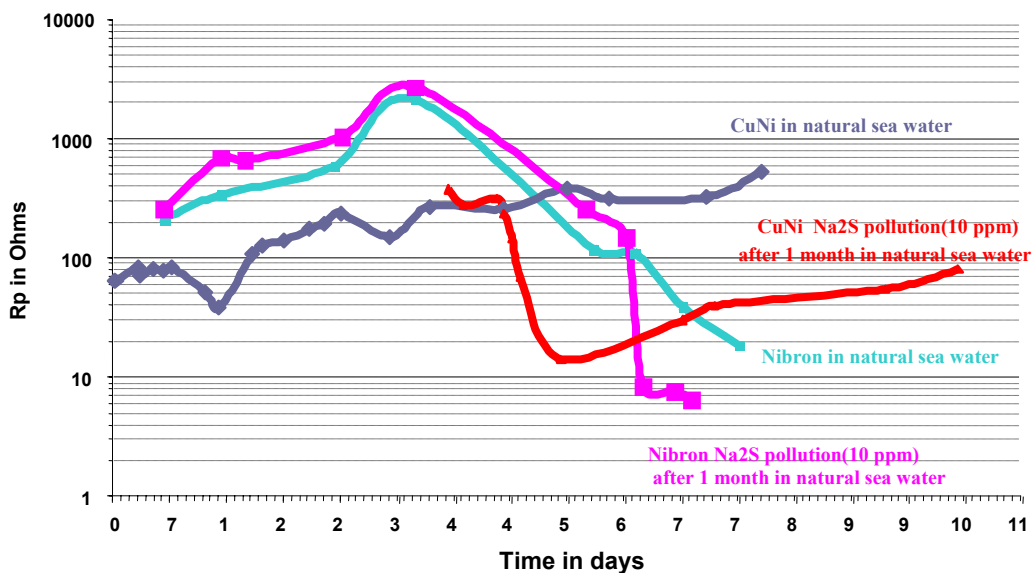


Figure 2 : Crevice Corrosion test bench under fretting



*Figure 3 : Eoc in natural sea water and polluted sea water with sulphides
Comparison between Nibron and CuNi10Fe1Mn*



*Figure4 : Rp in natural sea water and polluted sea water with sulphides
Comparison between Nibron and CuNi10Fe1Mn*

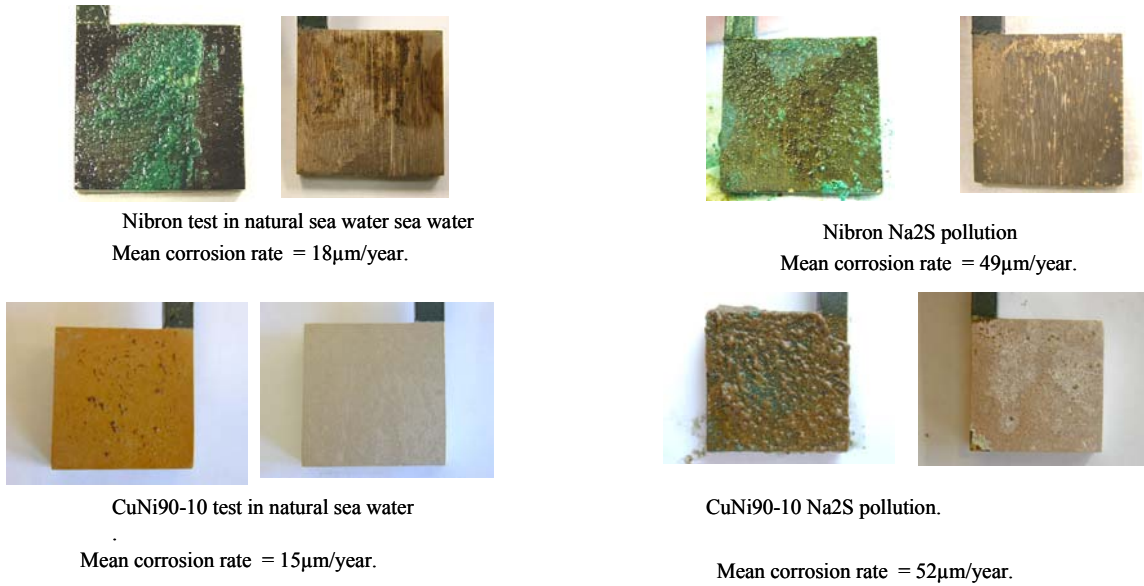


Figure 5 : Specimen examination after exposure to natural sea water and polluted sea water with sulphides
Comparison between Nibron and CuNi10Fe1Mn

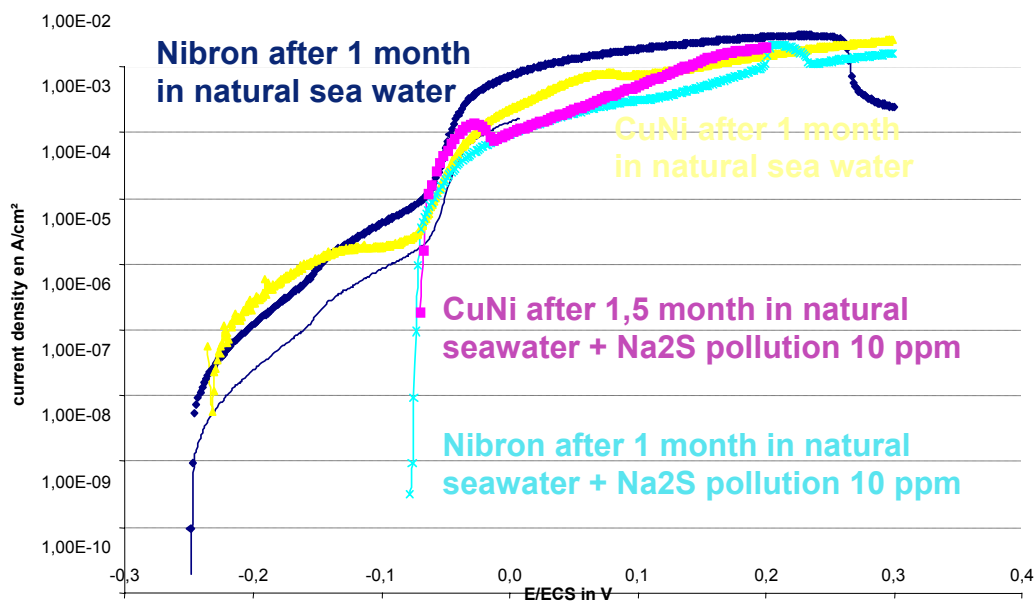


Figure 6: Anodic polarization curves after exposure to natural sea water and polluted sea water with sulphides
Comparison between Nibron and CuNi10Fe1Mn

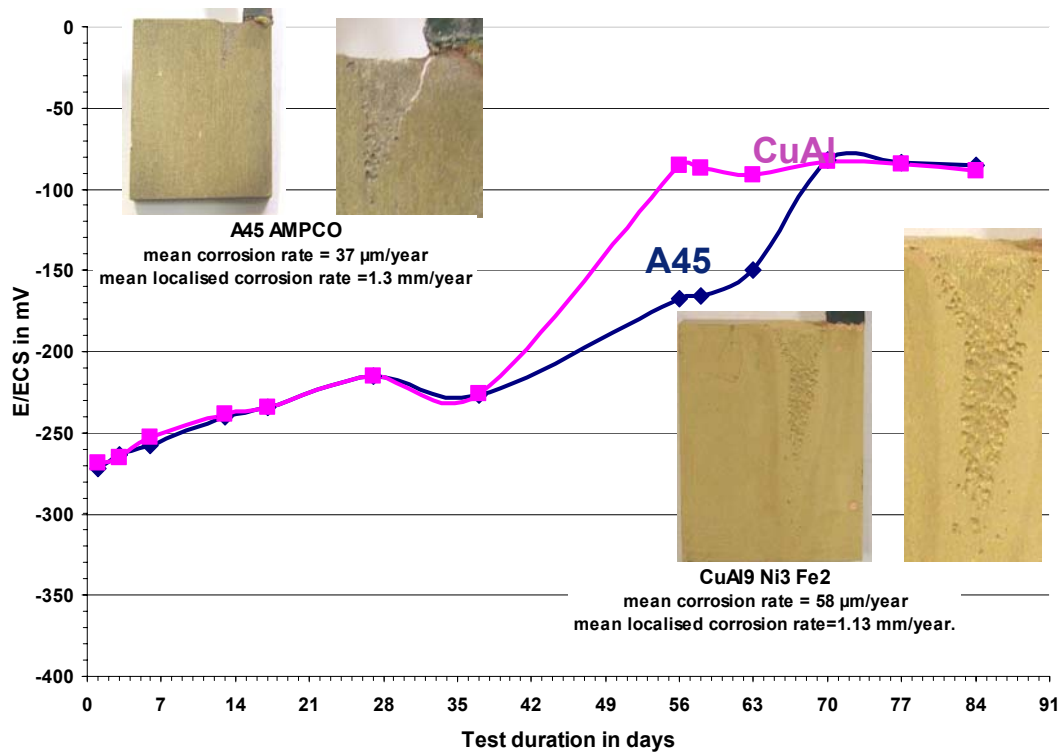


Figure 7: Eoc in natural sea water
 Comparison between A45 and CuAl9Ni3Fe2

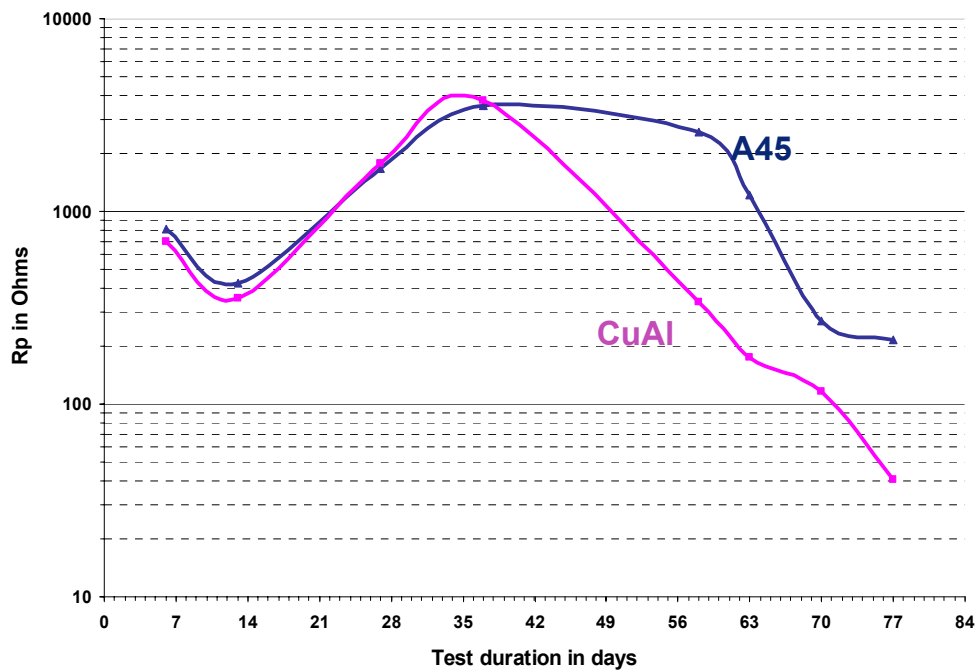


Figure 8: Rp in natural sea water-Comparison between A45 and CuAl9Ni3Fe2

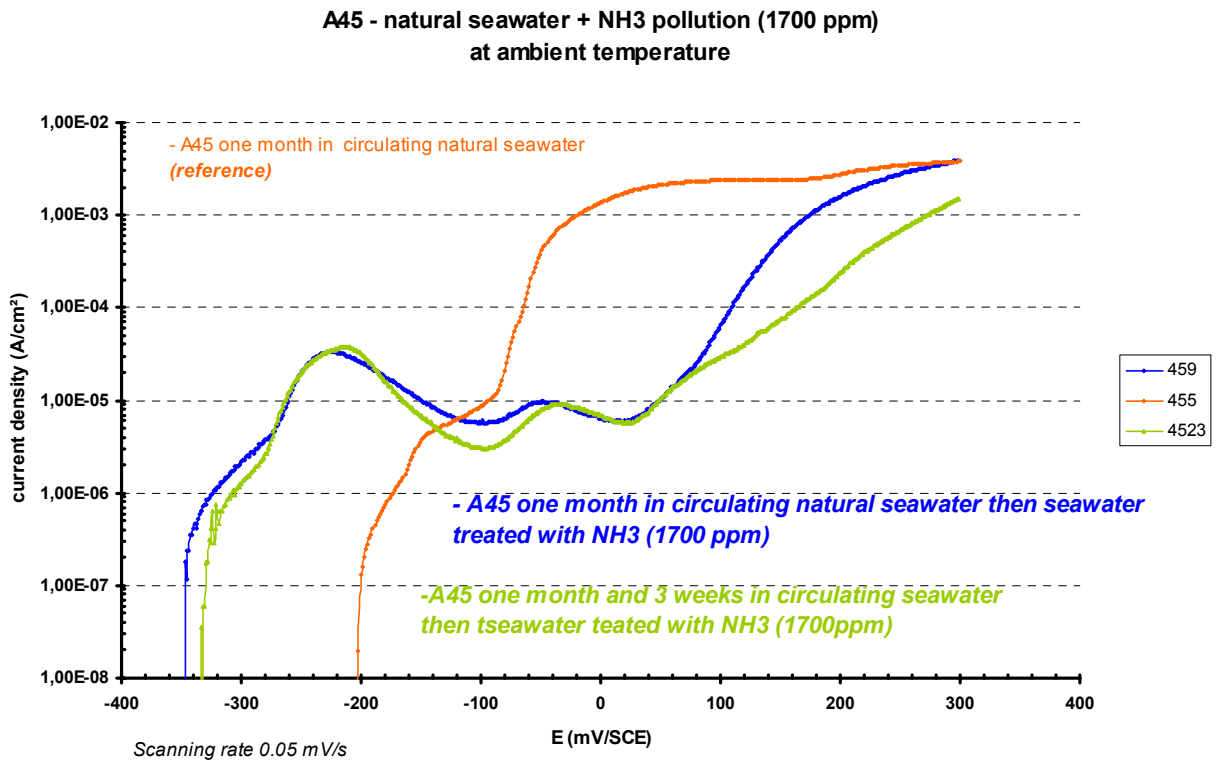


Figure 9: A45 Anodic polarization curves after exposure to natural sea water and polluted sea water with ammonia

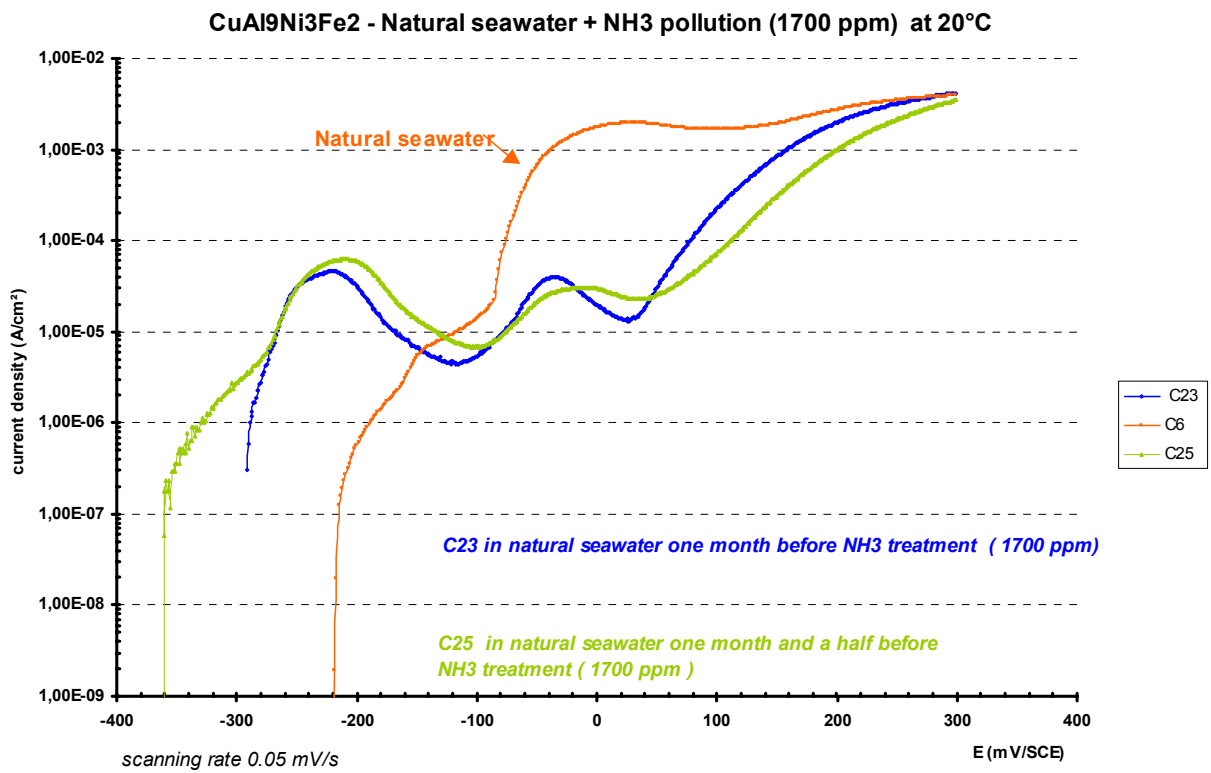


Figure 10: CuAl9Ni3Fe2 Anodic polarization curves after exposure to natural sea water and polluted sea water with ammonia

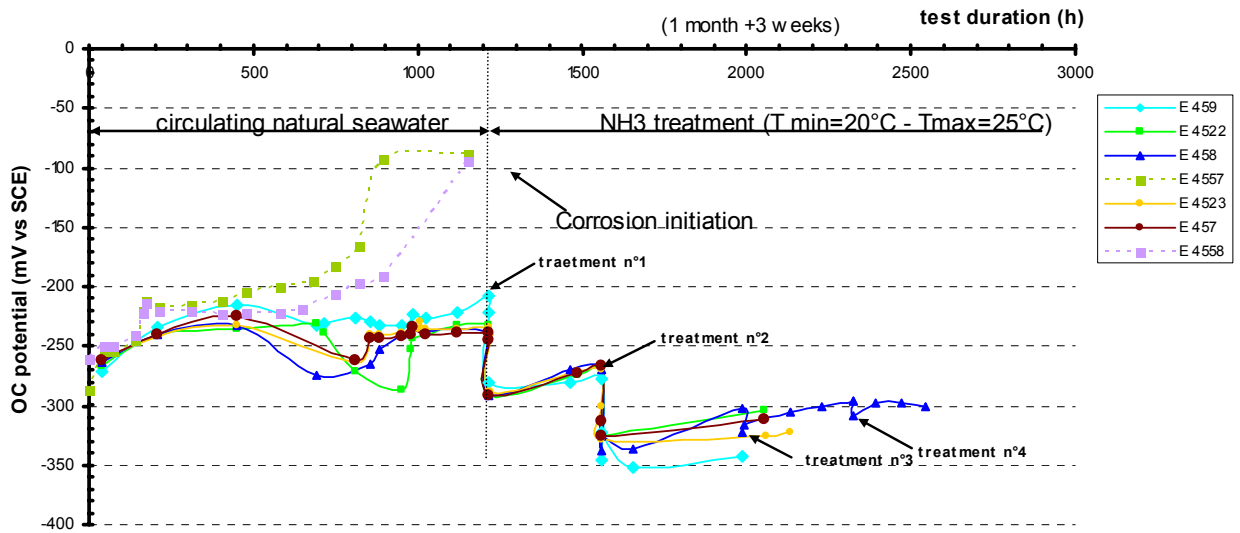


Figure 11: A45 Eoc in natural sea water and polluted sea water with ammonia

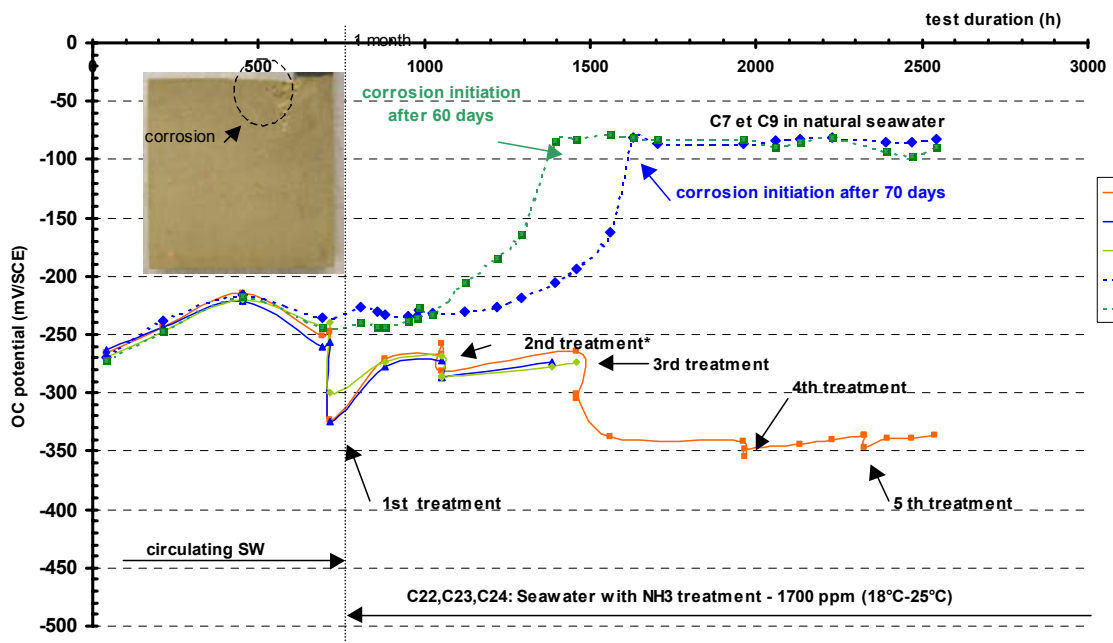


Figure 12: CuAl9Ni3Fe2 Eoc in natural sea water and polluted sea water with ammonia

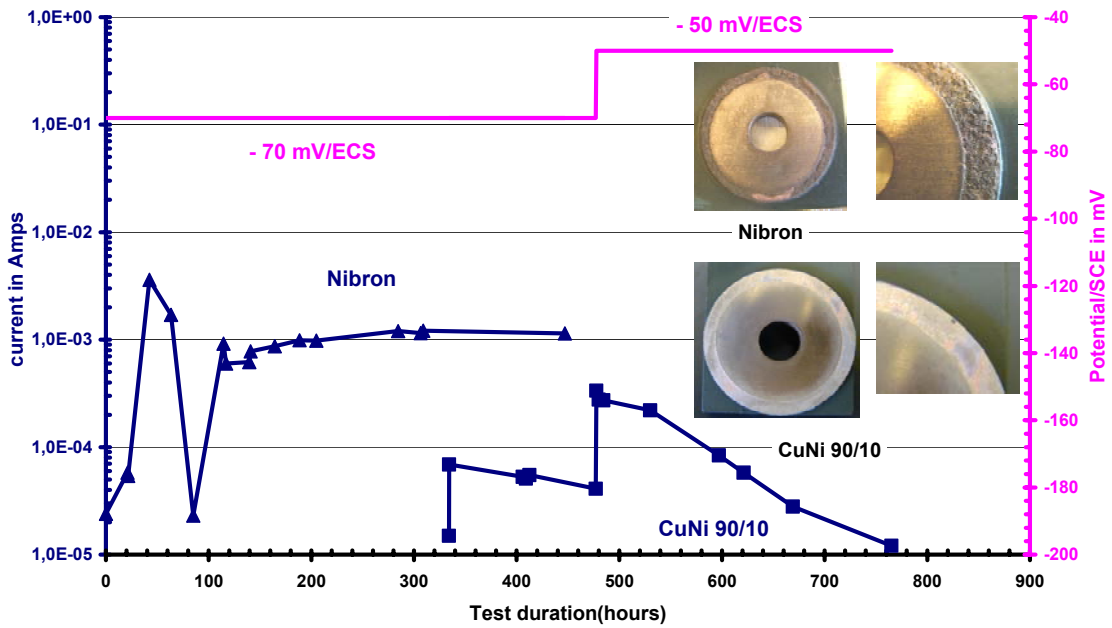


Figure 13
 Crevice corrosion initiation in natural sea water (ambient temperature)
 Comparison between Nibron and CuNi10Fe1Mn

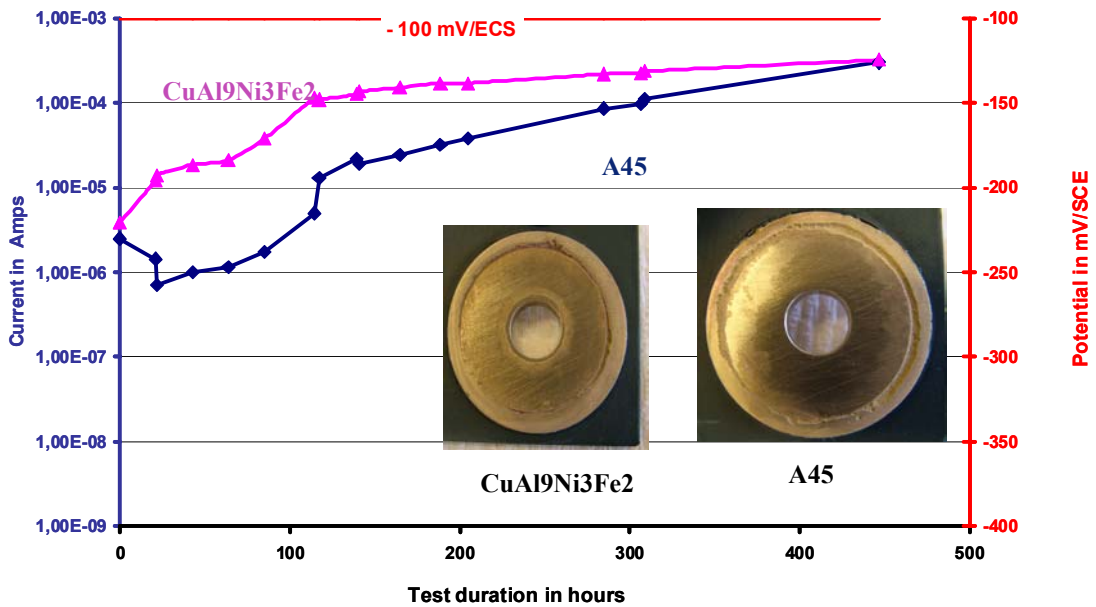


Figure 14
 Crevice corrosion initiation in natural sea water (ambient temperature)
 Comparison between A45 and CuAl9Ni3Fe2

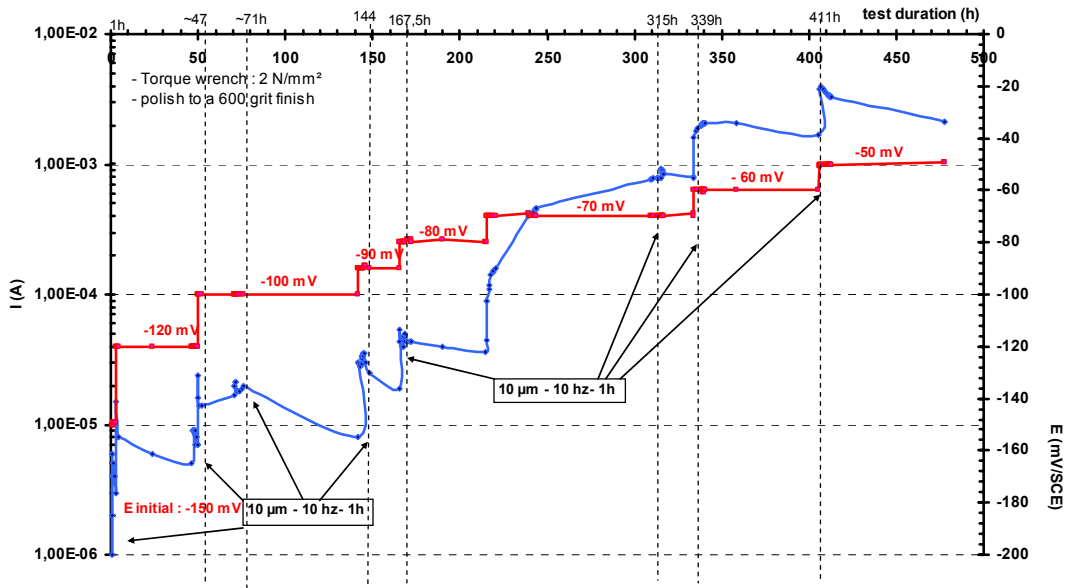


Figure 15 : Nibron - Crevice corrosion test under fretting in natural sea water 25°C

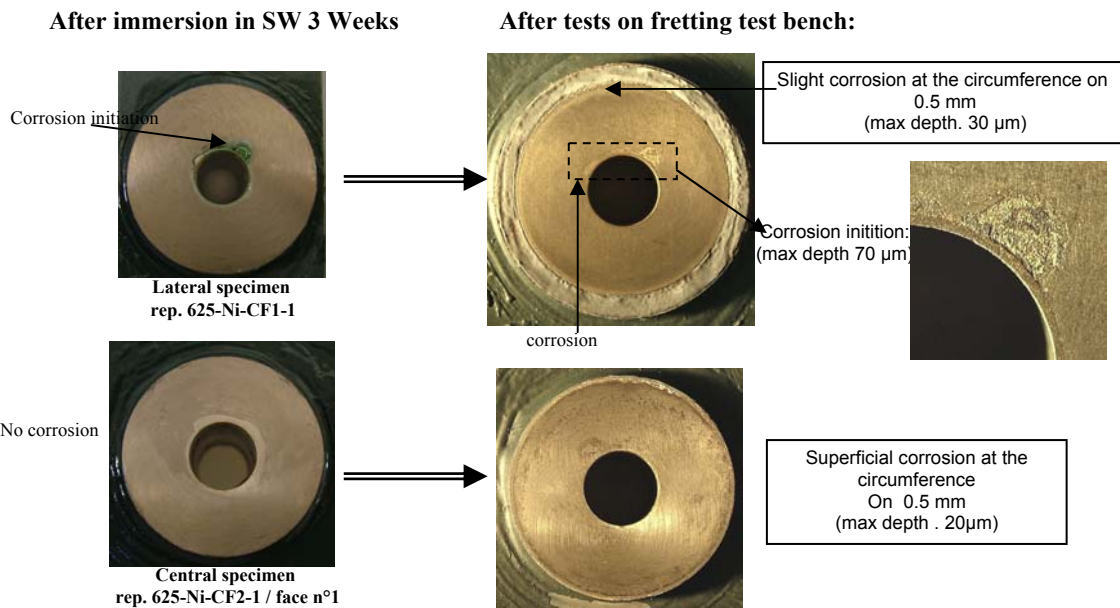


Figure 16 : Nibron – Specimen examination after crevice corrosion test under fretting in natural sea water (25°C)

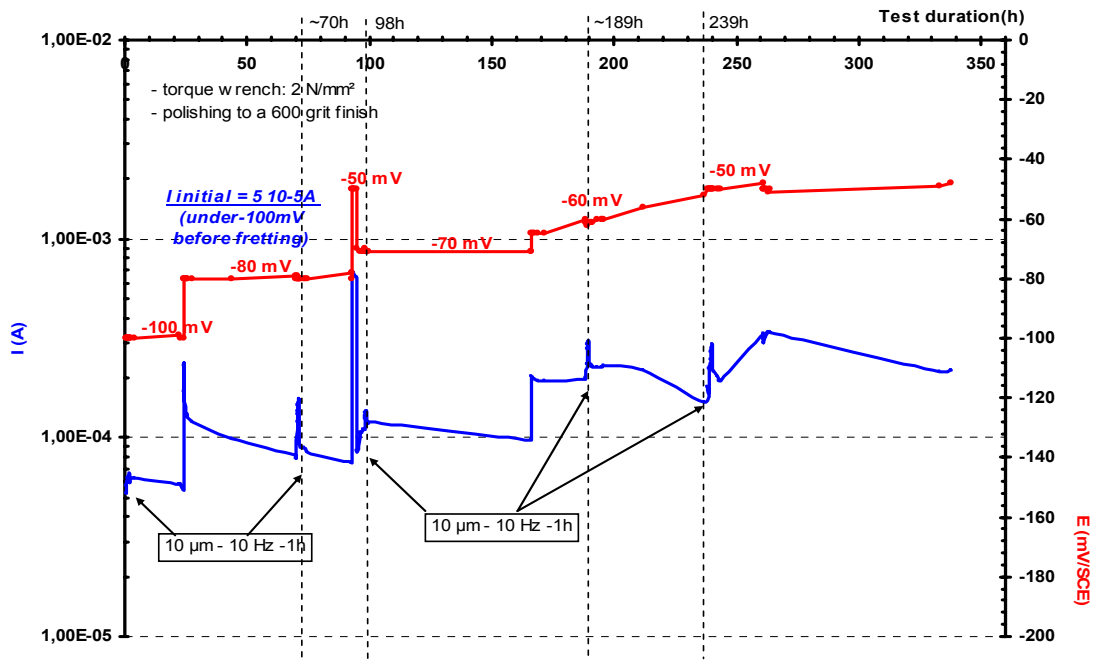


Figure 17 : CuNi10Fe1Mn - Crevice corrosion test under fretting in natural sea water 25°C

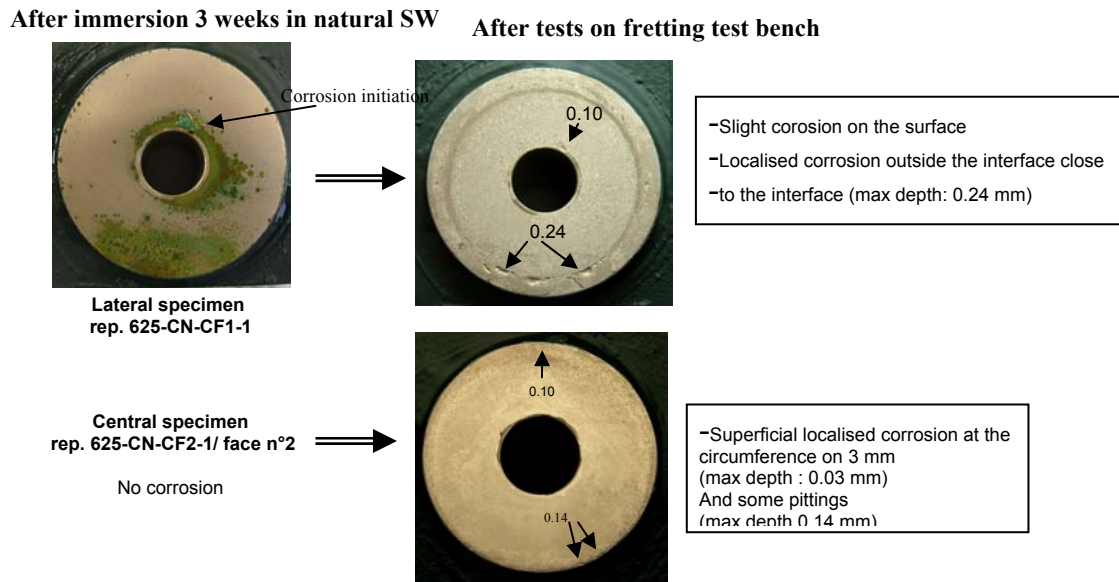


Figure 18 : CuNi10Fe1Mn – Specimen examination after crevice corrosion test under fretting in natural sea water (25°C)

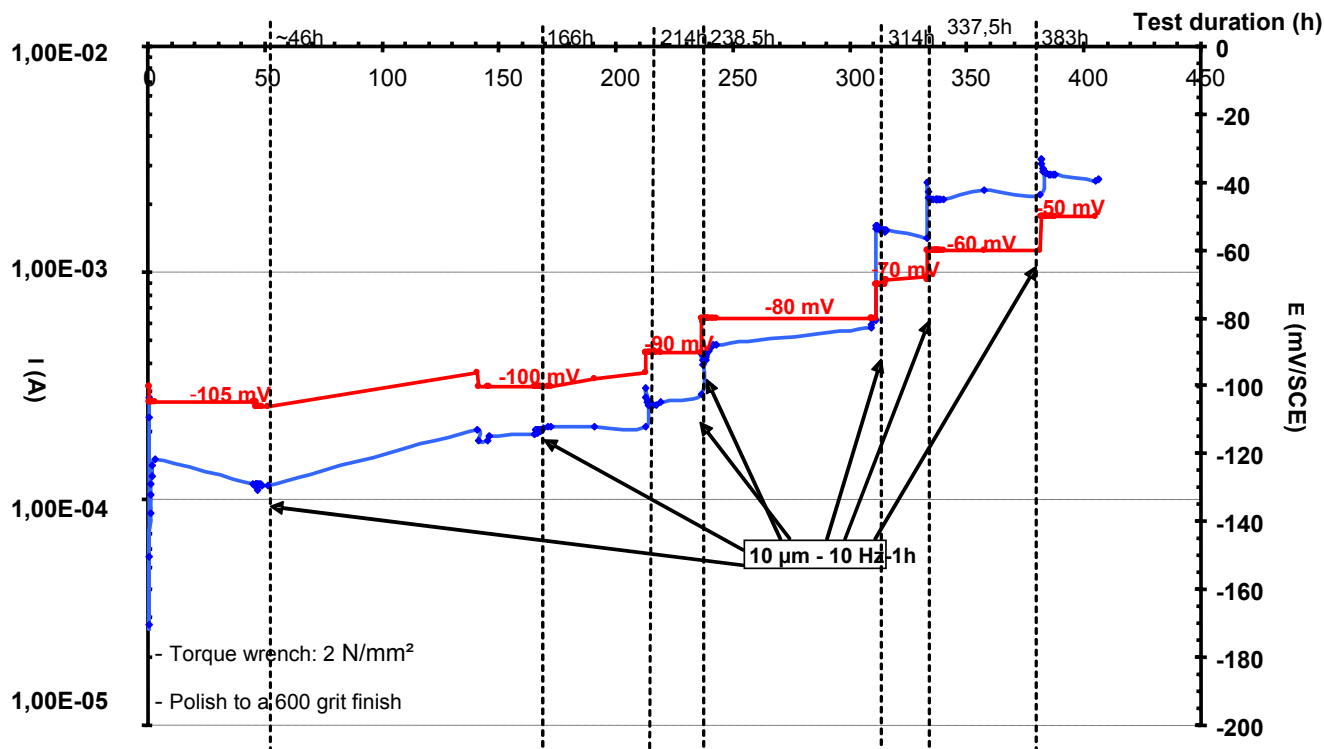


Figure 19: A45 - Crevice corrosion test under fretting in natural sea water 25°C

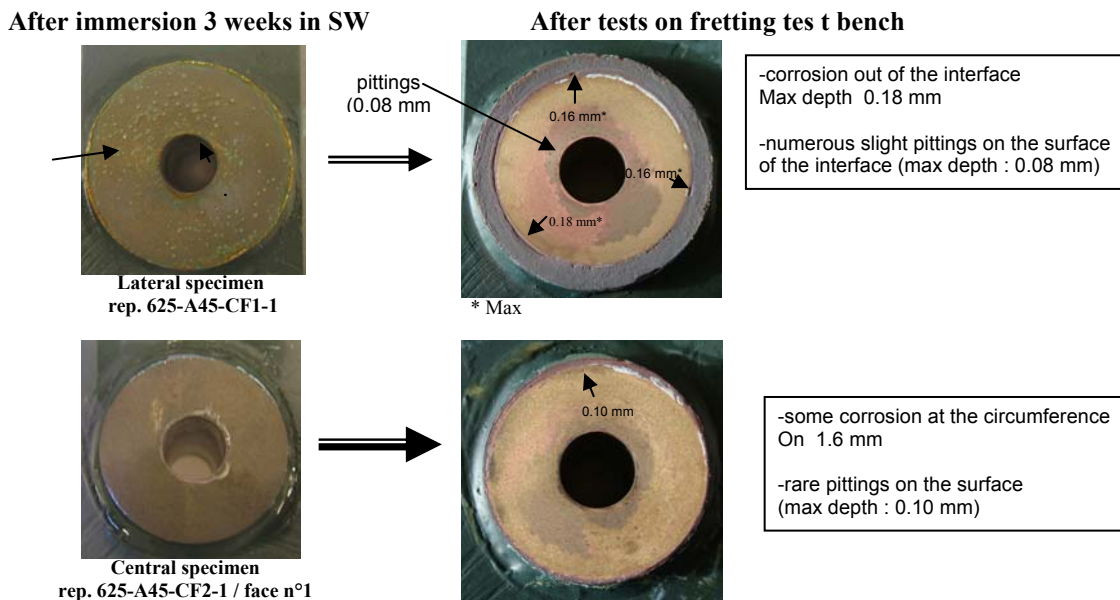


Figure 20: A45 – Specimen examination after crevice corrosion test under fretting in natural sea water (25°C)

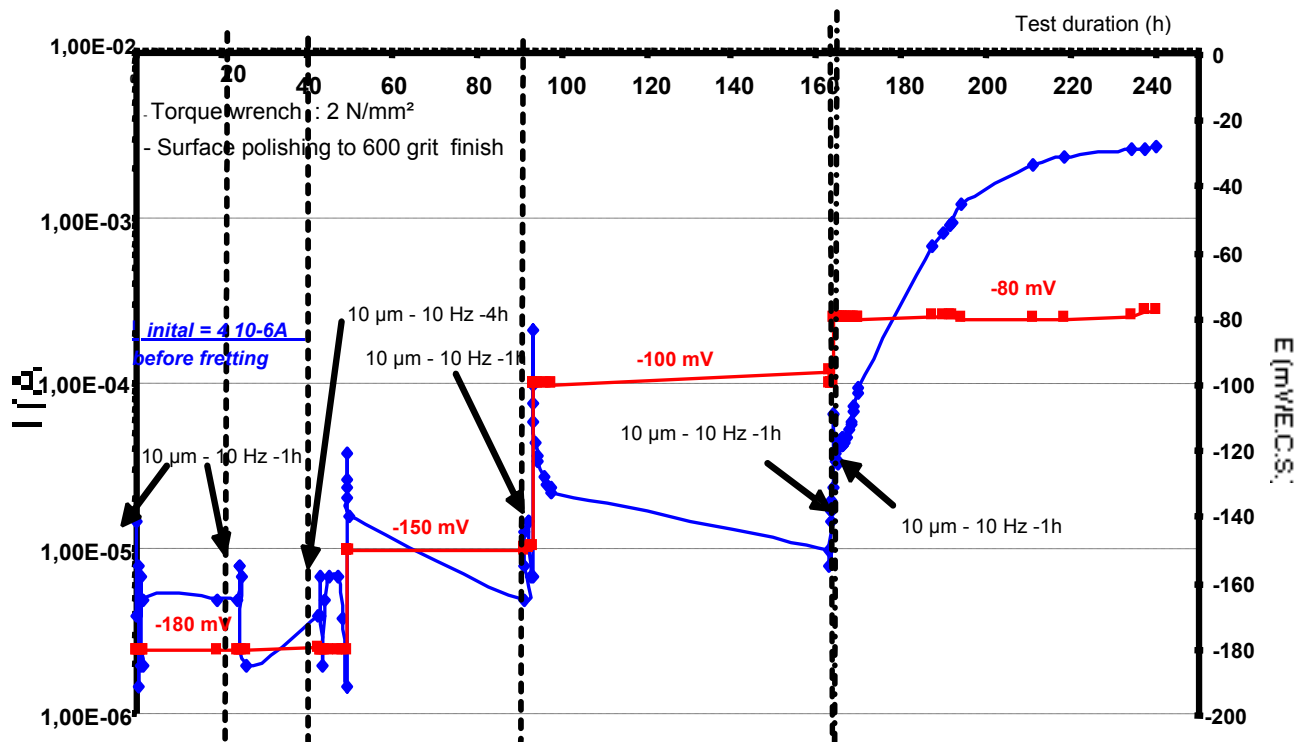


Figure 21 : CuAl9Ni3Fe2- Crevice corrosion test under fretting in natural sea water 25°C

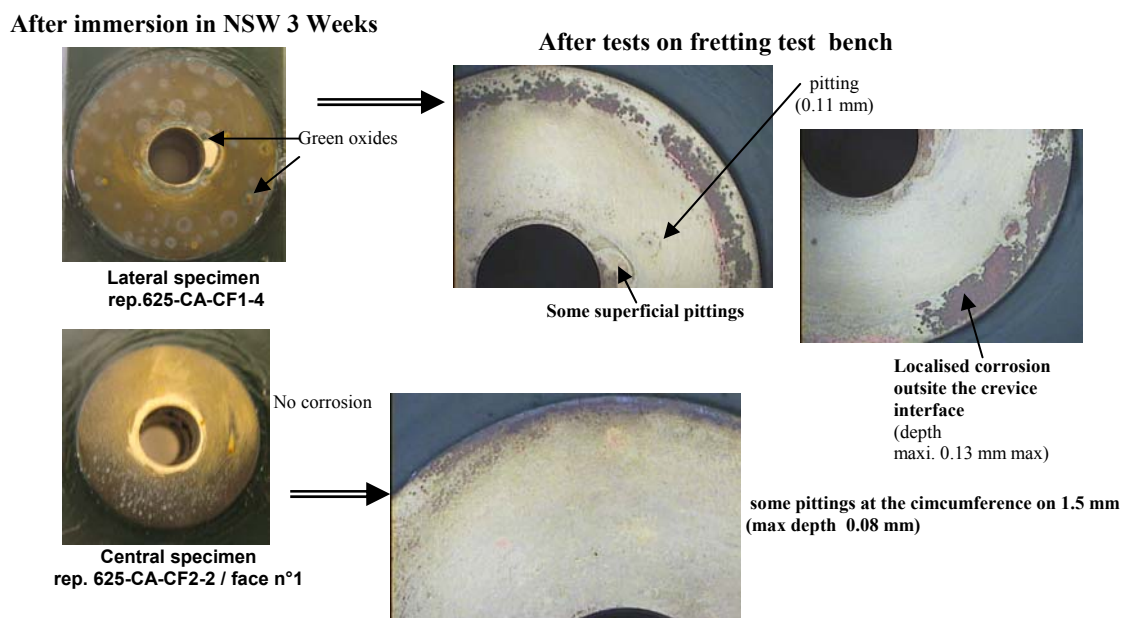


Figure 22 : CuAl9Ni3Fe2 – Specimen examination after crevice corrosion test under fretting in natural sea water (25°C)

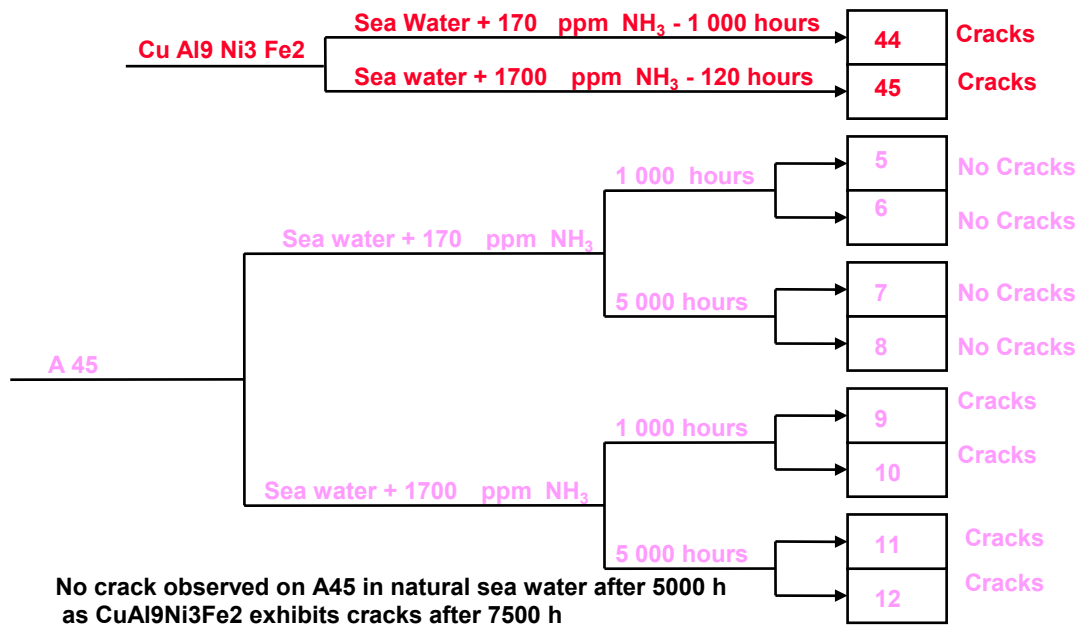


Figure 23 : A45 and CuAl9Ni3Fe2 -U-bend test results in natural sea water and polluted sea water with ammonia

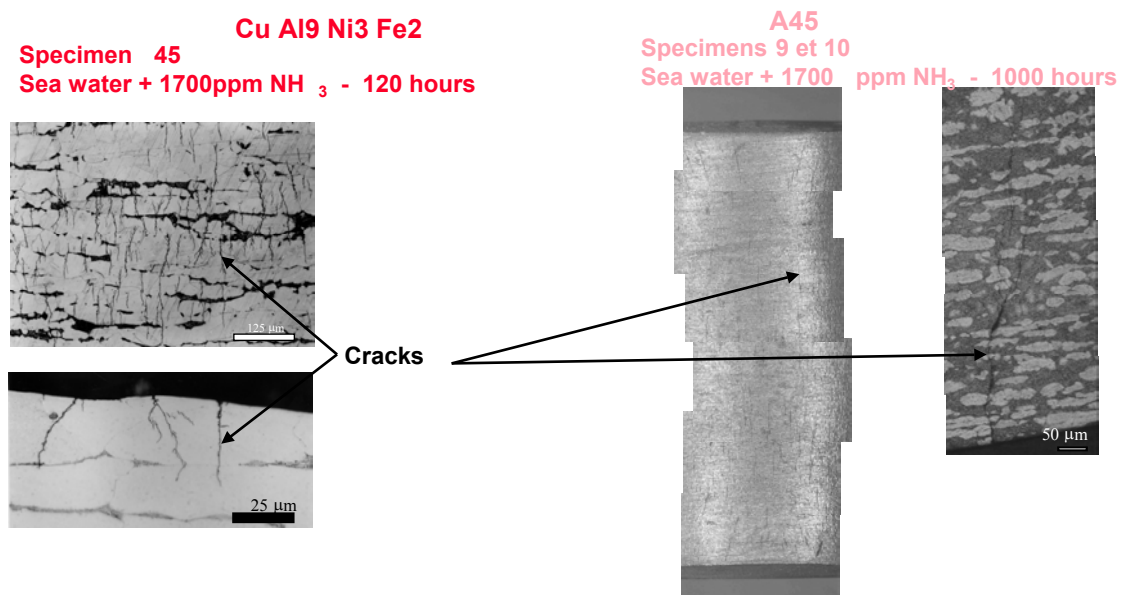


Figure 24: A45 and CuAl9Ni3Fe2 -U-bend test results in natural sea water and polluted sea water with ammonia- Specimen examinations

C Ni 90 - 10	Sea water + 170 ppm de NH_3 - 1 000	17 et	No cracks
	Sea water + 1700 ppm de NH_3 - 1 000	21 et	No cracks
	Sea water + 170 ppm de NH_3 - 5 000	19 et	No cracks
	Sea water + 1700 ppm de NH_3 - 5 000	23 et	No cracks
Nibron	Sea water + 170 ppm de NH_3 - 1 000	31 et	No cracks
	Sea water + 1700 ppm de NH_3 - 1 000	35 et	No cracks
	Sea water + 170 ppm de NH_3 - 5 000	33 et	No cracks
	Sea water + 1700 ppm de NH_3 - 5 000	37 et	No cracks

No cracks on CuNi 90-10 and Nibron observed after 5000 hours in natural sea water

Figure 25: Nibron and CuNi10Fe1Mn -U-bend test results in natural sea water and polluted sea water with ammonia-

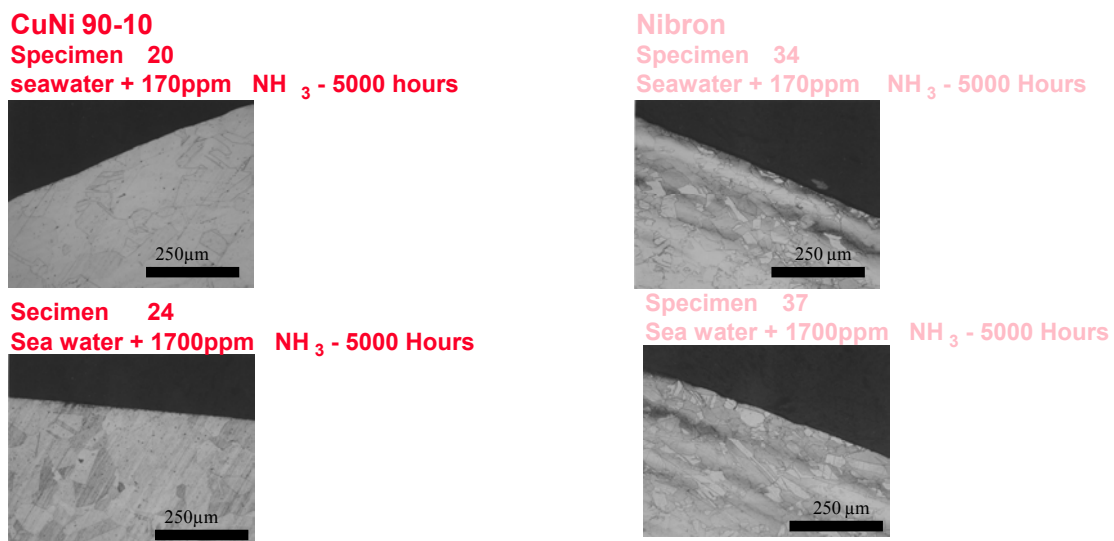


Figure 26: Nibron and CuNi10Fe1Mn -U-bend test results in natural sea water and polluted sea water with ammonia-Specimen examination